







Polaronic neutron in dilute α matter: A p -wave Bose polaronHiroyuki Tajima ^{1,2} Hajime Moriya,³ Tomoya Naito ^{4,1} Wataru Horiuchi ^{5,6,2,7} Eiji Nakano ⁸ and Kei Iida ^{8,2}¹*Department of Physics, Graduate School of Science, The University of Tokyo, Tokyo 113-0033, Japan*²*RIKEN Nishina Center, Wako 351-0198, Japan*³*Research Center for Nuclear Physics, Osaka University, Ibaraki 567-0047, Japan*⁴*Interdisciplinary Theoretical and Mathematical Science Program (iTHEMS), RIKEN, Wako 351-0198, Japan*⁵*Department of Physics, Osaka Metropolitan University, Osaka 558-8585, Japan*⁶*Nambu Yoichiro Institute of Theoretical and Experimental Physics (NITEP),**Osaka Metropolitan University, Osaka 558-8585, Japan*⁷*Department of Physics, Hokkaido University, Sapporo 060-0810, Japan*⁸*Department of Mathematics and Physics, Kochi University, Kochi 780-8520, Japan* (Received 30 August 2024; revised 24 November 2024; accepted 14 January 2025; published 5 February 2025)

We theoretically investigate quasiparticle properties of a neutron immersed in an alpha condensate, which is one of the possible states of dilute symmetric nuclear matter. The resonant p -wave neutron-alpha scattering, which plays a crucial role in forming halo nuclei, is considered. This system is similar to a Bose polaron near the p -wave Feshbach resonance that can be realized in cold-atomic experiments. Calculating the self-energy within the field-theoretical approach, we give an analytical formula for the effective mass of a polaronic neutron as a function of alpha condensation density. Moreover, two adjacent neutrons in a medium, each of which behaves like a stable polaron having an enhanced effective mass, can form a bound dineutron, with the help of 1S_0 neutron-neutron attraction. This is in contrast to the case of the vacuum, where a dineutron is known to be unbound. Our result is useful for understanding many-body physics in astrophysical environments as well as the formation of multinucleon clusters in neutron-halo nuclei.

DOI: [10.1103/PhysRevC.111.025802](https://doi.org/10.1103/PhysRevC.111.025802)**I. INTRODUCTION**

Infinite symmetric nuclear matter, where the proton charge is switched off, is fictitious but is one of the most fundamental nuclear systems because it is related to saturation of the binding energy and density of stable nuclei [1]. It is still interesting to consider infinite symmetric nuclear matter at relatively low densities, although, naively, the system is unstable to inhomogeneous phases at sufficiently low temperatures [2]. Once the proton charge is switched on, the nuclear liquid has to be a collection of nuclei. Furthermore, such symmetric matter can contain alpha particles via alpha clustering; indeed, some medium-heavy symmetric nuclei are predicted to be unstable with respect to alpha decay [3].

The nuclear equation of state and the composition in nuclear statistical equilibrium are important keys to understanding the mechanism of supernova explosions [4] and the dynamics of intermediate-energy heavy-ion collisions. To this end, dilute alpha matter and its Bose-Einstein condensation (BEC) phase have been studied as a good reference system for supernova matter at finite temperatures [5–8]. Alpha particles in such an astrophysical environment play a pivotal role in nucleosynthesis, e.g., triple-alpha reaction via the Hoyle state [9]. Moreover, the alpha condensates have also been discussed in the context of excited states of atomic nuclei [10,11], which are expected to be present in intermediate energy heavy-ion

collisions. However, the many-nucleon and dynamical nature of the systems of interest here leads to a lot of uncertainties and model dependencies.

To explore the aforementioned alpha clustering properties more clearly, various low-energy nuclear experiments have been performed. The existence of the alpha condensates has been examined experimentally such as ^{16}O [12] and ^{20}Ne [13]. In addition, experimental explorations of multinucleon clusters in nuclei of large neutron excess are ongoing [14–17]. While the existence of the tetra-neutron resonance has been discussed based on few-body calculations with multinucleon interactions [18–20] (see also the review [21]), it is known that the neutron-nucleus interaction plays a crucial role in the formation of halo nuclei [22]. There are several examples of two-neutron halo nuclei: ^6He [23], ^{11}Li [24], ^{14}Be [25], ^{19}B [26], ^{22}C [27–30], and ^{29}F [31,32]. Moreover, a recent experiment indicates that dineutron correlations play a crucial role in understanding the cluster structure of ^8He [33,34]. In between, neutrons and alpha clusters are expected to coexist; alpha clusters in a neutron-skin region of stable tin isotopes with small neutron excess have recently been identified by a knockout experiment [35].

Generally, to understand how the properties of an impurity particle change in medium from those in the vacuum, the notion of a polaron, which was originally proposed to see the properties of mobile electrons in ionic lattices [36,37], is useful. This is the case with nuclear systems in which

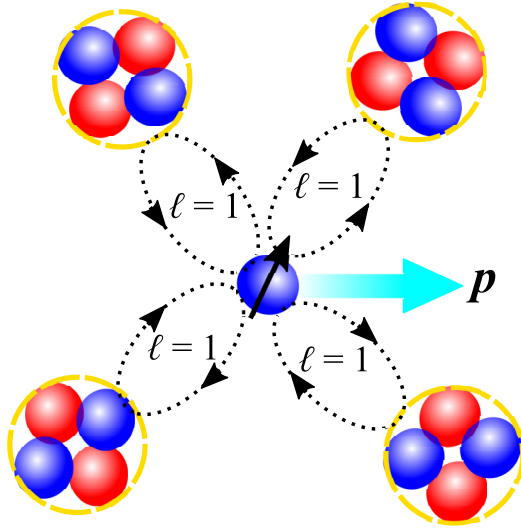


FIG. 1. Schematic picture of a polaronic neutron moving with momentum p in an alpha condensate, which is characterized by the neutron-alpha $J^\pi = 3/2^-$ p -wave resonance (i.e., relative angular momentum $\ell = 1$).

the medium and impurity particles can be single nucleons or nucleon composites (nuclear clusters). Polarons are now one of the hot topics in cold-atomic physics because of their tunable setup in recent experiments [38]. Some of the present authors clarified the quasiparticle properties of impurity protons and alpha particles in dilute neutron matter as encountered in the crust of a neutron star, in terms of Fermi polarons [39–42] (i.e., impurities immersed in a Fermi sea). In this regard, it is interesting to consider how neutrons are affected by alpha matter, as shown in Fig. 1, which can be relevant to intermediate energy heavy-ion collisions, stellar collapse, and the neutron-skin region of atomic nuclei. Indeed, a similar situation, that is, an impurity surrounded by BEC, is realized in cold-atomic systems as a so-called Bose polaron. Accordingly, the microscopic properties of Bose polarons have been extensively studied experimentally [43–46] and theoretically [47–55] (see also the review [56]).

In this paper, we theoretically investigate the quasiparticle properties of a neutron immersed in the alpha-condensate state of dilute symmetric nuclear matter, as schematically depicted in Fig. 1. We focus on the resonant $J^\pi = 3/2^-$ p -wave neutron-alpha coupling, which is responsible for the halo structure of neutron-rich nuclei such as ${}^6\text{He}$ [22]. In this regard, the system we are interested in is similar to Bose polarons near the p -wave Feshbach resonance, which would be experimentally accessible in several Bose-Fermi mixtures (e.g., ${}^6\text{Li}$ - ${}^{87}\text{Rb}$ [57], ${}^{40}\text{K}$ - ${}^{41}\text{K}$ [58], ${}^{23}\text{Na}$ - ${}^{40}\text{K}$ [59], and ${}^6\text{Li}$ - ${}^{133}\text{Cs}$ [60]). This system is different from the one treated in the previous work on polaronic neutrons in spin-polarized neutron matter [61–63]. While p -wave Fermi polarons have been investigated theoretically [64,65], their bosonic counterpart has yet to be addressed. It is still noteworthy that recently, the role of interspecies p -wave interactions has been discussed in the context of a magnon in a two-dimensional Bose-Bose mixture [66]. Here, we analyze the polaronic neu-

tron excitation by calculating the self-energy for the resonant p -wave neutron-alpha scattering. Furthermore, by considering the residual 1S_0 neutron-neutron attractive interaction, we study the fate of two adjacent polaronic neutrons in dilute alpha matter. The possible occurrence of bound dineutrons due to the polaron effect, which is explored by solving the Bethe-Salpeter equation, may be relevant to the formation of multinucleon clusters in neutron-rich nuclei, intermediate energy heavy-ion collisions, and core-collapse supernova cores. Moreover, in the presence of such a bound state, the crossover from dineutron BEC to Bardeen-Cooper-Schrieffer (BCS) neutron superfluid can be anticipated [67].

This paper is organized as follows: In Sec. II, the theoretical model and the Bose-polaron formalism are presented. In Sec. III, we show the result for the polaronic neutron excitations and then discuss the dineutron formation in the alpha condensate. A summary of this paper is given in Sec. IV.

II. FORMALISM

Hereinafter, we take $\hbar = k_B = 1$, and the system volume is set to unity.

A. Model

Here, we employ the two-channel Hamiltonian [68] for the $J^\pi = 3/2^-$ ${}^5\text{He}$ resonance, which is relevant at low relative energies, as given by

$$H = H_v + H_\alpha + H_\Phi + V_{3/2^-}, \quad (1)$$

where the contribution of spin-1/2 neutrons ($s_z = \pm 1/2$) with a mass M_v reads

$$\begin{aligned} H_v = & \sum_{s_z} \sum_{\mathbf{k}} \xi_{\mathbf{k},v} v_{\mathbf{k},s_z}^\dagger v_{\mathbf{k},s_z} \\ & + \sum_{\mathbf{k},\mathbf{k}',\mathbf{Q}} U_{2v}(\mathbf{k},\mathbf{k}') v_{\mathbf{k}+\mathbf{Q}/2,+1/2}^\dagger v_{-\mathbf{k}+\mathbf{Q}/2,-1/2}^\dagger \\ & \times v_{-\mathbf{k}'+\mathbf{Q}/2,-1/2} v_{\mathbf{k}'+\mathbf{Q}/2,+1/2} \end{aligned} \quad (2)$$

with the neutron kinetic energy $\xi_{\mathbf{k},v} = k^2/2M_v$, the neutron creation (annihilation) operator $v_{\mathbf{k},s_z}^\dagger$ ($v_{\mathbf{k},s_z}$), and the neutron-neutron coupling $U_{2v}(\mathbf{k},\mathbf{k}')$. The contribution of alpha particles reads

$$\begin{aligned} H_\alpha = & \sum_{\mathbf{q}} \xi_{\mathbf{q},\alpha} \alpha_{\mathbf{q}}^\dagger \alpha_{\mathbf{q}} \\ & + \frac{1}{2} \sum_{\mathbf{q},\mathbf{q}',\mathbf{K}} U_{2\alpha}(\mathbf{q},\mathbf{q}') \alpha_{\mathbf{q}+\mathbf{K}/2}^\dagger \alpha_{-\mathbf{q}+\mathbf{K}/2}^\dagger \\ & \times \alpha_{-\mathbf{q}'+\mathbf{K}/2} \alpha_{\mathbf{q}'+\mathbf{K}/2} \end{aligned} \quad (3)$$

with the alpha-particle kinetic energy $\xi_{\mathbf{q},\alpha} = q^2/2M_\alpha - \mu_\alpha$ ($M_\alpha = 4M_v$ and μ_α are the alpha particle mass and chemical potential, respectively), the alpha-particle annihilation (creation) operator $\alpha_{\mathbf{q}}^\dagger$ ($\alpha_{\mathbf{q}}$), and the alpha-alpha interaction $U_{2\alpha}(\mathbf{q},\mathbf{q}')$. The kinetic term of the closed-channel ${}^5\text{He}$ state with $J^\pi = 3/2^-$ ($J_z = \pm 1/2, \pm 3/2$) reads

$$H_\Phi = \sum_{P,J_z} (\xi_{P,\Phi} + E_\Phi) \Phi_{P,J_z}^\dagger \Phi_{P,J_z} \quad (4)$$

with the bare ${}^5\text{He}$ kinetic energy $\xi_{\mathbf{p},\Phi} = P^2/(2M_v + 2M_\alpha) - \mu_\alpha$, the bare ${}^5\text{He}$ energy level E_Φ , and the bare ${}^5\text{He}$ annihilation (creation) operator $\Phi_{\mathbf{p},J_z}^{(\dagger)}$. Note that we set the neutron chemical potential to zero since neutrons are regarded as impurities.

For a two-body system of a neutron with momentum \mathbf{p}_v and an alpha particle with momentum \mathbf{p}_α , using the center-of-mass momentum $\mathbf{P} = \mathbf{p}_v + \mathbf{p}_\alpha$ and the relative momentum $\mathbf{k} = M_r(\frac{\mathbf{p}_v}{M_v} - \frac{\mathbf{p}_\alpha}{M_\alpha})$ with the reduced mass $M_r^{-1} = M_v^{-1} + M_\alpha^{-1}$, one can rewrite \mathbf{p}_v and \mathbf{p}_α as

$$\mathbf{p}_v = \mathbf{k} + \frac{M_v}{M_v + M_\alpha} \mathbf{P} \equiv \mathbf{k} + \frac{\mathbf{P}}{5}, \quad (5)$$

$$\mathbf{p}_\alpha = -\mathbf{k} + \frac{M_\alpha}{M_v + M_\alpha} \mathbf{P} \equiv -\mathbf{k} + \frac{4\mathbf{P}}{5}, \quad (6)$$

respectively. Then, the interaction term $V_{3/2^-}$ responsible for the $J^\pi = 3/2^-$ p -wave resonance is given by

$$V_{3/2^-} = \sum_{J_z, s_z, m} \sum_{\mathbf{P}, \mathbf{k}} \left(kg_k \sqrt{\frac{4\pi}{3}} Y_m^{\ell=1}(\hat{\mathbf{k}}) \langle 1, m; 1/2, s_z | 3/2, J_z \rangle \right. \\ \left. \times \Phi_{\mathbf{p}, J_z}^\dagger v_{\mathbf{k}+\mathbf{P}/5, s_z} \alpha_{-\mathbf{k}+4\mathbf{P}/5} + \text{H.c.} \right), \quad (7)$$

where $\langle 1, m; 1/2, s_z | 3/2, J_z \rangle$ is the Clebsch-Gordan coefficient [69]. We employ the Yamaguchi-type form factor

$$gk = \frac{g}{1 + (k/\Lambda)^2}, \quad (8)$$

where Λ is the cutoff scale and g is the coupling strength at $k = 0$. These parameters are related to the low-energy constants as [68]

$$a_p = -\frac{M_r g^2}{6\pi} \left(E_\Phi - \frac{M_r g^2 \Lambda^3}{12\pi} \right)^{-1}, \\ r_p = -\frac{6\pi}{M_r^2 g^2} + \frac{24\pi E_\Phi}{M_r g^2 \Lambda^2} - 3\Lambda. \quad (9)$$

Here, $a_p = -67.1 \text{ fm}^3$ and $r_p = -0.87 \text{ fm}^{-1}$ are the $J^\pi = 3/2^-$ p -wave scattering volume and effective range, respectively [39]. Also, we set $\Lambda = 0.90 \text{ fm}^{-1}$ in such a way as to reproduce the ${}^5\text{He}$ resonance energy $E_{\text{res}} \simeq 0.93 \text{ MeV}$. We can then determine $E_\Phi = 449.607 \text{ MeV}$ and $M_r g^2 = 113.388 \text{ fm}^2$ from the empirical values of a_p and r_p .

B. Bose-polaron self-energy

As for a medium of dilute symmetric nuclear matter, we consider a zero-temperature alpha condensate. The alpha condensate density denoted by ρ_α controls the polaronic properties of an impurity neutron. Within the mean-field approximation, the alpha condensation energy density reads $\mathcal{E}_\alpha = -\mu_\alpha \rho_\alpha + \frac{1}{2} U_{2\alpha}(\mathbf{0}, \mathbf{0}) \rho_\alpha^2$, from which we obtain $\mu_\alpha = U_{2\alpha}(\mathbf{0}, \mathbf{0}) \rho_\alpha$. However, since the value of $U_{2\alpha}(\mathbf{0}, \mathbf{0})$ has a large uncertainty in the matter, for simplicity, we take $\mu_\alpha \simeq 0$, which is valid in the dilute regime. In this regard, the information on the alpha condensate is incorporated only via ρ_α .

We are interested in the neutron retarded Green's function

$$G_{s_z}(\mathbf{p}, \omega) = \frac{1}{\omega_+ - \xi_{\mathbf{p},v} - \Sigma_{s_z}(\mathbf{p}, \omega)}, \quad (10)$$

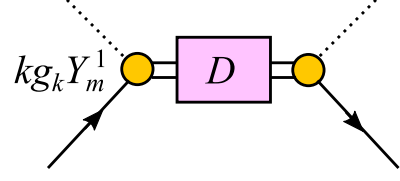


FIG. 2. Beliaev-type self-energy of a polaronic neutron in an alpha condensate, which is accompanied by the dressed ${}^5\text{He}$ propagator D . The dotted line describes the alpha condensate wave function or, equivalently, the square root of the condensate density $\sqrt{\rho_\alpha}$. The circles represent the neutron-alpha- ${}^5\text{He}$ coupling $kg_k Y_m^1$ within the $J^\pi = 3/2^-$ channel.

where $\omega_+ = \omega + i\delta$ involves an infinitesimally small imaginary number $i\delta$. Then, as diagrammatically shown in Fig. 2, the self-energy of a neutron embedded in the alpha condensate is given by the Beliaev-type diagram [47]:

$$\Sigma_{s_z}(\mathbf{p}, \omega) = \frac{4\pi}{3} \rho_\alpha \sum_{J_z} \sum_m \langle 1, m; 1/2, s_z | 3/2, J_z \rangle^2 \\ \times k^2 g_k^2 Y_m^1(\hat{\mathbf{k}}) [Y_m^1(\hat{\mathbf{k}})]^* D_{J_z}(\mathbf{p}, \omega), \quad (11)$$

which incorporates the resonant scattering between a neutron with momentum $\mathbf{p} = \mathbf{p}_v = \mathbf{k} + \mathbf{P}/5$ and an alpha particle with zero momentum $\mathbf{p}_\alpha = -\mathbf{k} + 4\mathbf{P}/5 = \mathbf{0}$ (i.e., in the condensate). In such a case, the relative momentum is given by

$$\mathbf{k} = \frac{1}{1 + \frac{M_v}{M_\alpha}} \mathbf{p} = \frac{4}{5} \mathbf{p}. \quad (12)$$

More explicitly, in the case of $s_z = +1/2$, we obtain

$$\Sigma_{1/2}(\mathbf{p}, \omega) = g_k^2 \rho_\alpha \left[\frac{k_x^2 + k_y^2}{2} D_{3/2}(\mathbf{p}, \omega) \right. \\ \left. + \frac{k_x^2 + k_y^2 + 4k_z^2}{6} D_{1/2}(\mathbf{p}, \omega) \right], \quad (13)$$

where the dressed ${}^5\text{He}$ propagators $D_{J_z}(\mathbf{p}, \omega)$ are given by

$$D_{J_z}(\mathbf{p}, \omega) = \frac{1}{\omega_+ - \xi_{\mathbf{p},\Phi} - E_\Phi - \Pi_{J_z}(\mathbf{p}, \omega)}. \quad (14)$$

Note that $\Sigma_{s_z=-1/2}(\mathbf{p}, \omega) = \Sigma_{s_z=1/2}(\mathbf{p}, \omega)$. The one-loop self-energy $\Pi_{J_z}(\mathbf{P}, \omega)$ for the neutron-alpha scattering reads

$$\Pi_{3/2}(\mathbf{P}, \Omega) = \sum_q g_q^2 \left(\frac{q_x^2 + q_y^2}{2} \right) \\ \times \frac{1}{\Omega_+ - \xi_{\mathbf{q}+\mathbf{P}/5,v} - \xi_{-\mathbf{q}+4\mathbf{P}/5,\alpha}}, \quad (15)$$

$$\Pi_{1/2}(\mathbf{P}, \Omega) = \sum_q g_q^2 \left(\frac{2}{3} q_z^2 + \frac{q_x^2 + q_y^2}{6} \right) \\ \times \frac{1}{\Omega_+ - \xi_{\mathbf{q}+\mathbf{P}/5,v} - \xi_{-\mathbf{q}+4\mathbf{P}/5,\alpha}}. \quad (16)$$

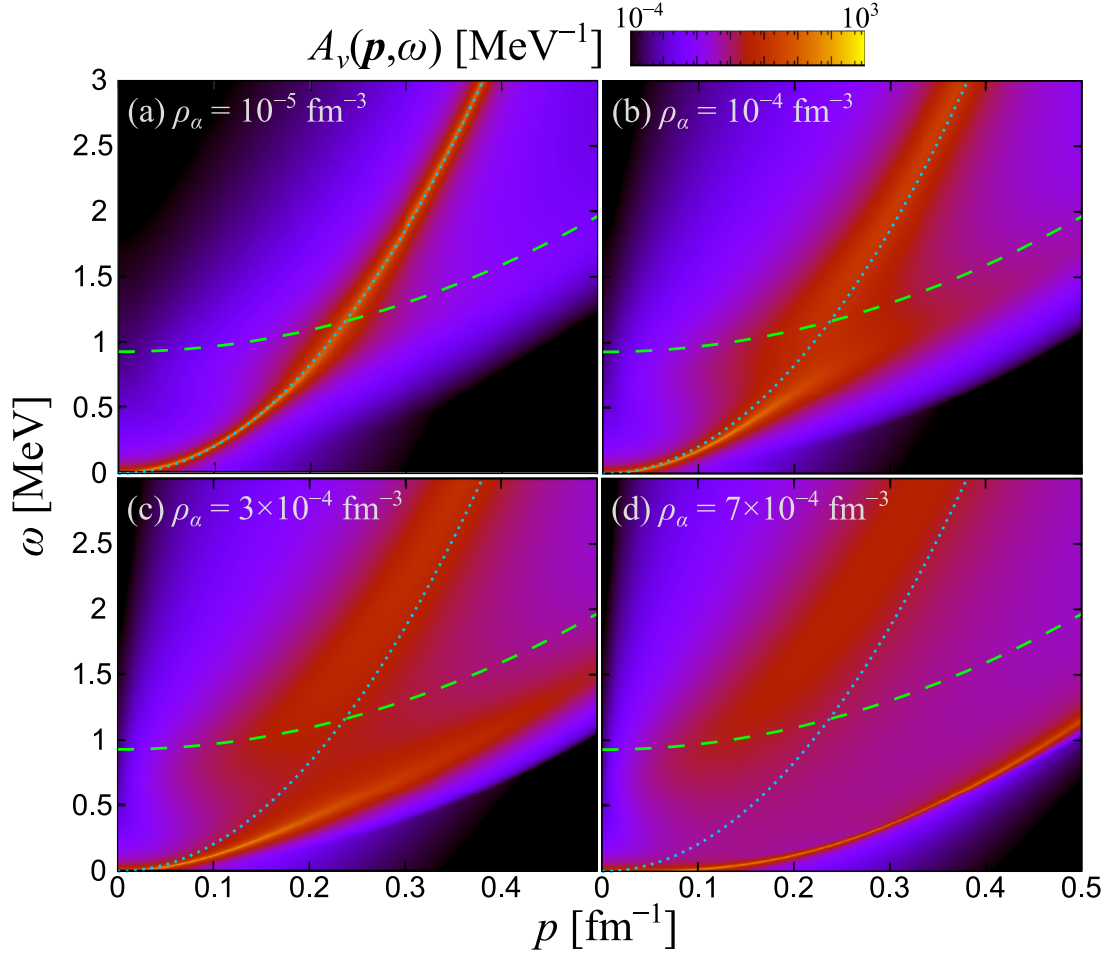


FIG. 3. Polaronic neutron spectral weight $A_v(\mathbf{p}, \omega)$ in the alpha condensate. For comparison, the bare neutron dispersion $\xi_{p,v} = p^2/2M_v$ (dotted curve) and ${}^5\text{He}$ resonance branch $p^2/(2M_v + 2M_\alpha) + E_{\text{res}}$ (dashed curve) are plotted in each panel. The alpha condensation densities are taken as (a) $\rho_\alpha = 10^{-5} \text{ fm}^{-3}$, (b) $\rho_\alpha = 10^{-4} \text{ fm}^{-3}$, (c) $\rho_\alpha = 3 \times 10^{-4} \text{ fm}^{-3}$, and (d) $\rho_\alpha = 7 \times 10^{-4} \text{ fm}^{-3}$.

Using $\xi_{q+P/5,v} + \xi_{-q+4P/5,\alpha} = q^2/2M_r + P^2/(2M_v + 2M_\alpha)$, we obtain $\Pi_{3/2}(\mathbf{P}, \Omega) = \Pi_{1/2}(\mathbf{P}, \Omega) = \Pi_0(\Omega_P)$ as

$$\Pi_0(\Omega_P) = -\frac{M_r g^2 \Lambda^4 [\Lambda^3 + 6\Lambda M_r \Omega_P + 2i(2M_r \Omega_P)^{3/2}]}{12\pi(2M_r \Omega_P + \Lambda^2)^2}, \quad (17)$$

with $\Omega_P = \Omega - P^2/(2M_v + 2M_\alpha)$. To obtain Eq. (17), we used $\sum_q q_j^2 F(q) = \frac{1}{3} \sum_q q^2 F(q)$ ($j = x, y, z$) for an arbitrary function $F(q = |\mathbf{q}|)$. Eventually, with $\omega_p = \omega - p^2/(2M_v + 2M_\alpha)$, we find

$$\Sigma_{s_z}(\mathbf{p}, \omega) = \frac{2}{3} \frac{k^2 g_k^2 \rho_\alpha}{\omega_+ - \xi_{p,\Phi} - E_\Phi - \Pi_0(\omega_p)}, \quad (18)$$

which is found to be isotropic in the momentum space, in contrast with Fermi polarons with anisotropic interactions [64,70].

III. RESULTS

Let us now exhibit numerical results for the properties of a Bose-polaronic neutron and the resultant implications for the bound dineutron.

A. Polaronic neutron in the alpha condensate

Figure 3 shows the polaronic neutron spectral weight given by

$$A_v(\mathbf{p}, \omega) = -\frac{1}{\pi} \text{Im} G_{s_z}(\mathbf{p}, \omega), \quad (19)$$

where we omitted the spin index $A_v(\mathbf{p}, \omega)$. For the overall structure, one can see that a sharp peak remains typically up to the threshold momentum of ${}^5\text{He}$ given by $\sqrt{2M_v E_{\text{res}}} \simeq 0.21 \text{ fm}^{-1}$ in the low-density regime. In the low-density regime, e.g., $\rho_\alpha = 10^{-5} \text{ fm}^{-3}$ in Fig. 3(a), one can see that the quasiparticle peak is located close to the bare dispersion $\xi_{p,v} = p^2/2M_v$ and that the spectral broadening occurs near the ${}^5\text{He}$ resonance. At $\rho_\alpha = 10^{-4} \text{ fm}^{-3}$, as shown in Fig. 3(b), there is a deviation between the spectral peak and the bare dispersion in such a way that the effective mass of the polaronic neutron branch becomes larger than the bare one. This can be understood as the avoided-crossing behavior of neutron quasiparticle and ${}^5\text{He}$ resonance branches. Moreover, the spectral broadening due to the coupling with the ${}^5\text{He}$ resonance branch is more prominent at larger alpha condensate densities, i.e., $\rho_\alpha = 3 \times 10^{-4} \text{ fm}^{-3}$ in Fig. 3(c).

Finally, just below a critical density $\rho_c = 7.41 \times 10^{-4} \text{ fm}^{-3}$ (which we derive below), as shown in Fig. 3(d) where we set $\rho_\alpha = 7 \times 10^{-4} \text{ fm}^{-3}$, the spectral weight is flattened in the low-momentum limit, which corresponds to the almost-divergent effective mass.

To examine the low-energy quasiparticle properties of a neutron immersed in the alpha condensate, we perform the low-momentum expansion of $\Sigma_{s_z}(\mathbf{p}, \omega)$. First, one can find

$$\Sigma_{s_z}(\mathbf{p} = \mathbf{0}, \omega) = 0, \quad (20)$$

because $\Sigma_{s_z}(\mathbf{p}, \omega)$ is always proportional to k^2 due to the p -wave properties. Accordingly, the p -wave polaron energy E_P is zero [i.e., $E_P = \Sigma_{s_z}(\mathbf{p} = \mathbf{0}, \omega) = 0$]. We expand $\Sigma_{s_z}(\mathbf{p}, \omega)$ around $\mathbf{p} = \mathbf{0}$ and $\omega = \xi_{p=0, v} = 0$ as

$$\begin{aligned} \Sigma_{s_z}(\mathbf{p}, \omega) &\simeq \Sigma_{s_z}(\mathbf{0}, \xi_{0, v}) + \left. \frac{\partial \Sigma_{s_z}(\mathbf{0}, \omega)}{\partial \omega} \right|_{\omega=\xi_{0, v}} (\omega - \xi_{0, v}) \\ &+ \frac{1}{2} \left. \frac{\partial^2 \Sigma_{s_z}(\mathbf{p}, \xi_{0, v})}{\partial p^2} \right|_{p=0} p^2. \end{aligned} \quad (21)$$

In this way, we obtain the approximate form of polaronic neutron Green's function

$$G_{s_z}(\mathbf{p}, \omega) \simeq \frac{Z}{\omega_+ - \frac{p^2}{2M_{\text{eff}}} + i\Gamma_P/2}, \quad (22)$$

where $\Sigma_{s_z}(\mathbf{0}, \xi_{0, v}) = 0$. Here, we define the quasiparticle residue

$$Z = \left[1 - \text{Re} \left. \frac{\partial \Sigma_{s_z}(\mathbf{0}, \omega)}{\partial \omega} \right|_{\omega=0} \right]^{-1} \quad (23)$$

and the inverse effective mass

$$\frac{M_v}{M_{\text{eff}}} = Z \left[1 + M_v \text{Re} \left. \frac{\partial^2 \Sigma_{s_z}(\mathbf{p}, \xi_{0, v})}{\partial p^2} \right|_{p=0} \right]. \quad (24)$$

The low-momentum expansion of $\Sigma_{s_z}(\mathbf{p}, \omega)$ reads

$$\Sigma_{s_z}(\mathbf{p}, \omega) = \frac{2}{3 \left(1 + \frac{M_v}{M_\alpha} \right)^2} \frac{g^2 \rho_\alpha p^2}{\omega_+ - E_\Phi - \Pi_0(\omega)} + O(p^4). \quad (25)$$

We analytically obtain $\Pi_0(0) = -M_r g^2 \Lambda^3 / 12\pi$ and hence

$$\left. \frac{\partial^2 \Sigma_{s_z}(\mathbf{p}, 0)}{\partial p^2} \right|_{p=0} = - \frac{8\pi a_p}{M_v \left(1 + \frac{M_v}{M_\alpha} \right)} \rho_\alpha. \quad (26)$$

Moreover, one can find

$$\frac{\partial \Sigma_{s_z}(\mathbf{0}, \omega)}{\partial \omega} = 0, \quad \rightarrow Z = 1, \quad (27)$$

$$\text{Im} \Sigma_{s_z}(\mathbf{0}, \omega) = 0, \quad \rightarrow \Gamma_P = 0. \quad (28)$$

Taking $Z \rightarrow 1$ in Eq. (24), we obtain

$$\frac{M_v}{M_{\text{eff}}} = 1 + \frac{8\pi M_\alpha a_p \rho_\alpha}{M_v + M_\alpha} < 1 \quad (a_p < 0), \quad (29)$$

indicating the heavier effective mass compared to the bare one. This enhancement can be understood as the level repulsion between quasiparticle neutron and ${}^5\text{He}$ branches where the quasiparticle neutron branch is pushed to lower energies

by the coupling with a broad ${}^5\text{He}$ resonance, as found in Fig. 3. Eventually, the formation of a bound dineutron in the alpha condensate is possible with the help of the induced interaction [71].

If the alpha-condensation density increases further, the effective mass diverges at

$$\rho_c = \frac{1}{8\pi |a_p|} \left(1 + \frac{M_v}{M_\alpha} \right) \simeq 7.41 \times 10^{-4} \text{ fm}^{-3}. \quad (30)$$

Beyond ρ_c , the effective mass of a polaronic neutron becomes negative, indicating a breakdown of the low-momentum polaron picture in the rest frame of the homogeneous alpha condensate and possibly a signature of self-localization of a polaronic neutron as discussed in Refs. [66,72,73]. This is in sharp contrast to p -wave Fermi polarons [64,65], of which a transition to a Feshbach molecular state was predicted to occur. We also note that the negative effective mass was discussed in repulsive Fermi polarons as a precursor of ferromagnetic instability [74]. Although we do not consider the alpha-alpha interaction and resulting quantum depletion explicitly—such effects would not drastically change the result for the effective mass. In fact, it is reported that the effective mass is not strongly affected by the boson-boson interaction in the case of s -wave Bose polarons [47].

Strictly speaking, however, the alpha-alpha interaction should affect various properties of the medium itself even at $\rho \approx \rho_c$. For example, $4\rho_c$ is not necessarily equal to the critical value of the total nucleon density because the depletion of the condensate due to quantum fluctuations occurs even at $T = 0$. Indeed, such a depletion is predicted to originate from the inter-alpha interactions and the in-medium breakup of alpha particles themselves [75]. Therefore, ρ_c may well be regarded as the critical density for the condensate component of alpha matter (not for the whole system). Then, the corresponding total nucleon density could be much higher than $4\rho_c$, which suggests that the system is more like a liquid state rather than a gas state as usually assumed in earlier investigations [76].

To see in more detail the structure of the neutron spectral weight, we plot $A_v(\mathbf{p}, \omega)$ at fixed momenta and different ρ_α in Fig. 4, where $p = 10^{-2} \text{ fm}^{-1}$ and $p = 10^{-1} \text{ fm}^{-1}$ are used in the Figs. 4(a) and 4(b), respectively. At a sufficiently small momentum, as shown in Fig. 4(a), a stable polaron peak can be found even near the critical density. On the other hand, at larger ρ_α , one can find a small peak of $A_v(\mathbf{p}, \omega)$ around the ${}^5\text{He}$ resonance ($E_{\text{res}} \simeq 0.93 \text{ MeV}$), implying the excited branch is associated with the level repulsion between the quasiparticle neutron and ${}^5\text{He}$ branches. Because the width of the ${}^5\text{He}$ resonance ($\simeq 0.6 \text{ MeV}$) is substantially broad in the present energy scale [68], however, this peak is also largely broadened. At larger frequencies, the neutron spectral weight monotonically decreases. Building the high-frequency limit of Eq. (17),

$$\Pi_0(\omega \rightarrow \infty) \rightarrow -i \frac{M_r g^2 \Lambda^4}{6\pi \sqrt{2M_r \omega}}, \quad (31)$$

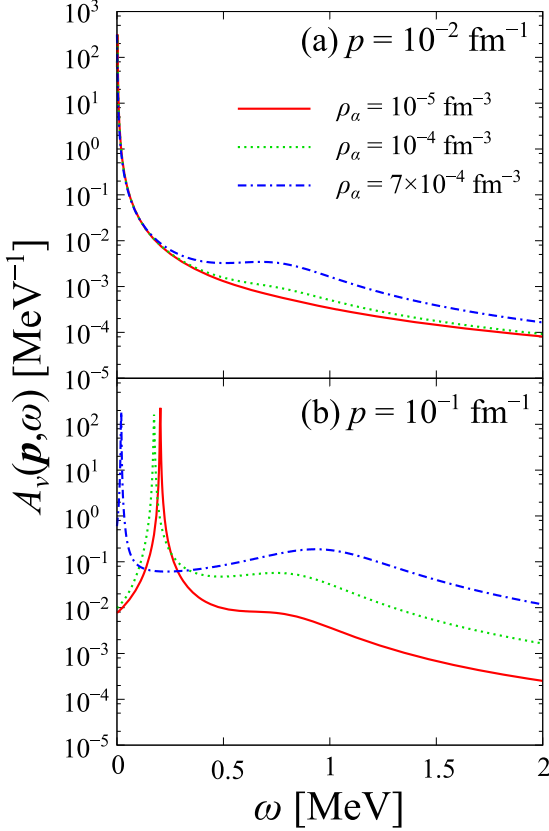


FIG. 4. Polaronic neutron spectral weight $A_v(\mathbf{p}, \omega)$ with fixed momentum (a) $p = 10^{-2} \text{ fm}^{-1}$ and (b) $p = 10^{-1} \text{ fm}^{-1}$ in the alpha condensate.

into $\text{Im}\Sigma_{s_z}(\mathbf{p}, \omega \rightarrow \infty)$ as

$$\begin{aligned} \text{Im}\Sigma_{s_z}(\mathbf{p}, \omega \rightarrow \infty) &\rightarrow \frac{2g^2\rho_\alpha k^2 \text{Im}\Pi_0(\omega \rightarrow \infty)}{3\omega^2} + O(k^4) \\ &\equiv -\frac{M_r g^4 \Lambda^4 \rho_\alpha p^2}{9\pi^2 \sqrt{2M_r} \left(1 + \frac{M_n}{M_\alpha}\right)^2 \omega^{9/2}} + O(p^4), \end{aligned} \quad (32)$$

we obtain the high-frequency tail of the spectral weight at low momenta as

$$A_v(\mathbf{p}, \omega \rightarrow \infty) \rightarrow \frac{M_r g^4 \Lambda^4 \rho_\alpha p^2}{9\pi^2 \sqrt{2M_r} \left(1 + \frac{M_n}{M_\alpha}\right)^2 \omega^{9/2}} + O(p^4), \quad (33)$$

indicating that the high-frequency tail is proportional to ρ_α as well as p^2 . Indeed, Fig. 4(a) shows the enhancement of the high-frequency spectra with increasing ρ_α . As shown in Fig. 4(b), at a larger momentum, the polaron peak is shifted toward high frequencies in such a way as to follow the dispersion relation $p^2/2M_{\text{eff}}$ at relatively small ρ_α . We remark in passing that, in a manner consistent with the p dependence of Eq. (33), the high-frequency contribution in Fig. 4(b) is significantly larger than that in Fig. 4(a).

B. Dineutrons in the alpha condensate

Here, we show that a dineutron can be a bound state due to the enhanced M_{eff} together with the 1S_0 neutron-neutron interaction $U_{2\nu}(k, k')$. A similar binding mechanism of two alpha particles in dilute neutron matter has been examined theoretically [40]. On the basis of the results of the polaronic neutron spectra shown in Fig. 3, we employ the approximated form of the polaronic neutron propagator in dilute alpha matter as

$$\tilde{G}_{s_z}(\mathbf{p}, \omega) \simeq \frac{\theta(k_c - p)}{\omega_+ - p^2/2M_{\text{eff}}} + \frac{\theta(p - k_c)}{\omega_+ - p^2/2M_\nu}, \quad (34)$$

where we have assumed that the low-energy polaron state is valid up to some momentum cutoff k_c . Equation (34) imitates two branches induced by the avoided crossing of neutron quasiparticle and ${}^5\text{He}$ resonance branches except for the region near $\rho_\alpha = \rho_c$. In this work, we specifically focus on the role of the enhanced neutron effective mass at low momenta below k_c found in Fig. 3. The precise value of k_c , which is controlled by the properties of the alpha condensate and the neutron-alpha interaction, remains to be known, and hence will be taken arbitrarily in the range of $0.1 \text{ fm}^{-1} \lesssim k_c \lesssim 10 \text{ fm}^{-1}$. While the spectral broadening due to the coupling with the ${}^5\text{He}$ resonance should also be important above $k = k_c$, we consider two bare neutrons in a virtual state there for simplicity because we are interested in the ground state of the two-neutron system in the alpha condensate, where the low-momentum properties, namely, enhanced effective masses, play a pivotal role. We note that the higher-momentum properties of neutrons would be important when neutrons undergo the Fermi degeneracy at finite excess neutron densities.

The two-neutron T -matrix $T_{2\nu}(k, k', \Omega)$ in the 1S_0 channel is given by

$$\begin{aligned} T_{2\nu}(k, k', \Omega) &= U_{2\nu}(k, k') + i \sum_q \int_{-\infty}^{\infty} \frac{d\omega}{2\pi} U_{2\nu}(k, q) \\ &\quad \times \tilde{G}_{+1/2}(\mathbf{q}, \omega + \Omega) \tilde{G}_{-1/2}(-\mathbf{q}, -\omega) \\ &\quad \times T_{2\nu}(q, k', \Omega). \end{aligned} \quad (35)$$

Using the separable 1S_0 neutron-neutron interaction $U_{2\nu}(k, k') = U_0 \chi_k \chi_{k'}$ with the form factor χ_k to be specified below, we obtain $T_{2\nu}(k, k'; \Omega) = t_{2\nu}(\Omega) \chi_k \chi_{k'}$ with

$$t_{2\nu}(\Omega) = \frac{U_0}{1 - U_0 \Xi(\Omega)}, \quad (36)$$

where the polarization function Ξ reads

$$\Xi(\Omega) = \sum_q \frac{\chi_q^2 \theta(k_c - q)}{\Omega_+ - q^2/M_{\text{eff}}} + \sum_q \frac{\chi_q^2 \theta(q - k_c)}{\Omega_+ - q^2/M_\nu}, \quad (37)$$

with $\Omega_+ = \Omega + i\delta$. The dineutron binding energy $E_{2\nu}$ can be obtained from

$$1 - U_0 \Xi(\Omega = -E_{2\nu}) = 0. \quad (38)$$

Practically, we use $\chi_q = 1/\sqrt{1 + (q/\lambda)^2}$. The parameters U_0 and λ are determined by the 1S_0 scattering length $a_{2\nu} = -18.5 \text{ fm}$ and $r_{2\nu} = 2.8 \text{ fm}$ as [77]

$$U_0 = \frac{4\pi a_{2\nu}}{M_\nu} \frac{1}{1 - a_{2\nu}\lambda}, \quad \lambda = \frac{1}{r_{2\nu}} \left(1 + \sqrt{1 - \frac{2r_{2\nu}}{a_{2\nu}}}\right). \quad (39)$$

Moreover, one can perform the momentum summation in Eq. (37) as

$$\Xi(-E_{2\nu}) = -\frac{M_\nu \lambda^2}{2\pi^2} \left[\frac{M_{\text{eff}} \lambda \tan^{-1}\left(\frac{k_c}{\lambda}\right) - \sqrt{M_{\text{eff}} E_{2\nu}} \tan^{-1}\left(\frac{k_c}{\sqrt{M_{\text{eff}} E_{2\nu}}}\right)}{M_\nu (\lambda^2 - M_{\text{eff}} E_{2\nu})} + \frac{\pi}{2} \frac{1}{\lambda + \sqrt{M_\nu E_{2\nu}}} - \frac{\lambda \tan^{-1}\left(\frac{k_c}{\lambda}\right) - \sqrt{M_\nu E_{2\nu}} \tan^{-1}\left(\frac{k_c}{\sqrt{M_\nu E_{2\nu}}}\right)}{\lambda^2 - M_\nu E_{2\nu}} \right]. \quad (40)$$

In this way, the bound-state equation reads

$$1 - \frac{1}{a_{2\nu} \lambda} = \frac{2}{\pi} \left[\frac{M_{\text{eff}} \tan^{-1}\left(\frac{k_c}{\lambda}\right) - \sqrt{\frac{M_{\text{eff}} M_\nu E_{2\nu}}{\lambda^2}} \tan^{-1}\left(\frac{k_c}{\lambda} \sqrt{\frac{M_\nu \lambda^2}{M_{\text{eff}} M_\nu E_{2\nu}}}\right)}{M_\nu (1 - \frac{M_{\text{eff}} M_\nu E_{2\nu}}{\lambda^2})} + \frac{\pi}{2} \frac{1}{1 + \sqrt{\frac{M_\nu E_{2\nu}}{\lambda^2}}} - \frac{\tan^{-1}\left(\frac{k_c}{\lambda}\right) - \sqrt{\frac{M_\nu E_{2\nu}}{\lambda^2}} \tan^{-1}\left(\frac{k_c}{\lambda} \sqrt{\frac{\lambda^2}{M_\nu E_{2\nu}}}\right)}{1 - \frac{M_\nu E_{2\nu}}{\lambda^2}} \right]. \quad (41)$$

The numerical results for $E_{2\nu}$ that can be obtained from Eq. (41) are shown in Fig. 5. These results indicate that dineutrons can be bound due only to the effective-mass acquisition of polaronic neutrons and the direct 1S_0 neutron-neutron interaction, even without the help of the medium-induced interaction. In this case, there is a threshold effective mass $M_{\text{eff},c}$ for the presence of a bound dineutron, which can be obtained by taking $E_{2\nu} = 0$ in Eq. (41) as

$$\frac{M_{\text{eff},c}}{M_\nu} = 1 - \frac{\pi}{2a_{2\nu} \lambda \tan^{-1}\left(\frac{k_c}{\lambda}\right)}. \quad (42)$$

Here, one needs to examine the cutoff-parameter dependence of $E_{2\nu}$ and $M_{\text{eff},c}$. As shown in Fig. 5, where several different values of k_c/λ are taken with λ fixed at 0.765 fm^{-1} [see Eq. (40)], $E_{2\nu}$ increases with k_c . This is

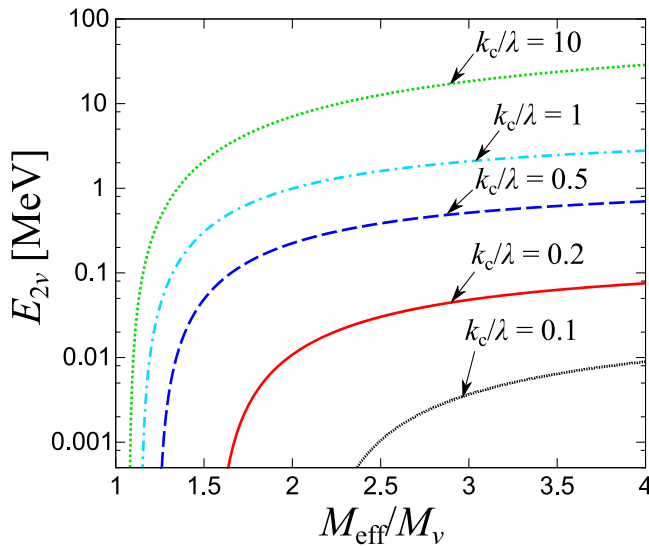


FIG. 5. Dineutron binding energy $E_{2\nu}$ in dilute alpha matter as a function of the effective mass M_{eff} of a polaronic neutron with various values of the cutoff parameter k_c divided by $\lambda = 0.765 \text{ fm}^{-1}$.

because, for larger k_c , each neutron more often behaves like a polaronic massive particle; according to Eq. (41), for $k_c \gg \lambda$, where $\tan^{-1}(k_c/\lambda) \simeq \pi/2$, $E_{2\nu}$ is close to its upper limit $\lambda^2/M_{\text{eff}}[(M_{\text{eff}}/M_\nu)/(1 - 1/a_{2\nu}\lambda) - 1]^2$, while for $k_c \ll \lambda$, where $\tan^{-1}(k_c/\lambda) \simeq k_c/\lambda$, the condition for $E_{2\nu} > 0$ is sensitive to the value of k_c . Also, $M_{\text{eff},c}$ tends to decrease with increasing k_c , as is clear from Eq. (42). While the notable k_c dependence of $E_{2\nu}$ can be found in Fig. 5, it would be fair to employ $k_c/\lambda = 0.2$ (i.e., $k_c \simeq 0.15 \text{ fm}^{-1}$), below which the polaronic spectral weight exhibits a sharp quasiparticle peak, as shown in Figs. 3(a) and 3(b).

In Fig. 6, we show the effective mass M_{eff} of a polaronic neutron as a function of ρ_α . For comparison, we also show the critical effective mass $M_{\text{eff},c}$ for the formation of a bound dineutron in the alpha condensate in the case of $k_c/\lambda = 0.2$. In this case, a bound dineutron starts to appear around $\rho_\alpha \simeq 3 \times 10^{-4} \text{ fm}^{-3}$, where polaronic neutrons remain stable and become sufficiently massive. Such kind of formation of bound dineutrons might be relevant to the alpha and dineutron clustering structure of neutron-rich light nuclei such as ^8He [33] and ^{10}Be [78,79]. While the condensation density ρ_α is substantially lower than the normal nuclear density, as already discussed in the previous subsection, ρ_α could be substantially lower than the total alpha density, including the effects of quantum depletion. Also, the dineutron formation in the alpha condensate via the neutron-alpha p -wave coupling is similar to the structure of two-neutron halo nuclei such as ^6He and ^{11}Li . To take a closer look at this similarity, the $J^\pi = 1/2^-$ channel as neglected in the present study would have to be taken into account.

IV. SUMMARY

In this paper, we have investigated the properties of a polaronic neutron in dilute alpha matter; the Bose polaron picture adopted here has been extensively examined in cold-atomic physics. We have shown that each polaronic neutron undergoes a large enhancement of the effective mass, a

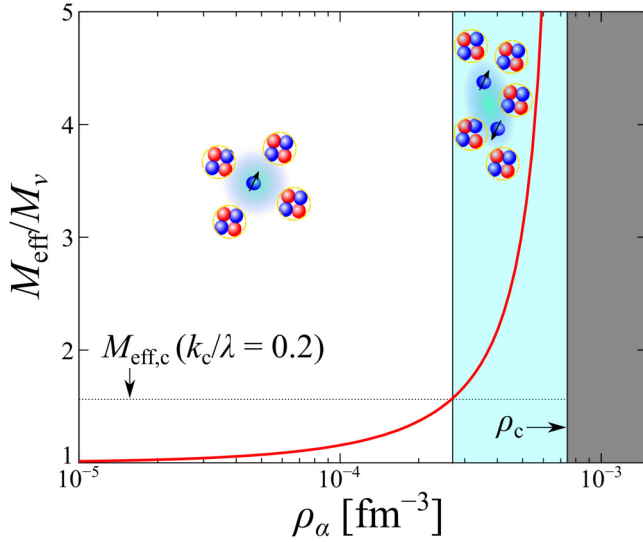


FIG. 6. Effective mass M_{eff} of a polaronic neutron plotted as a function of the alpha condensation density ρ_α . The horizontal dotted line shows the critical effective mass $M_{\text{eff},c}$ for the presence of a bound dineutron in the case of $k_c/\lambda = 0.2$; for momenta below this k_c , a sharp peak can be seen in the calculated neutron spectral weight. In the shaded region beyond the critical alpha condensation density ρ_c given by Eq. (30), the polaronic neutron experiences divergence of the effective mass, indicating the breakdown of the low-momentum polaron picture in the rest frame of the alpha condensate and possibly the resultant self-localization [66,72,73].

vanishing decay, and a constant quasiparticle residue, because of the resonant p -wave coupling with the alpha condensate. Such effective mass enhancement helps to form bound dineutrons, together with the 1S_0 neutron-neutron attraction, which is not sufficiently strong to induce the dineutron binding in the vacuum.

To examine more quantitative properties of bipolaronic dineutrons, effects of spectral broadening, finite neutron density and temperature, the alpha-mediated interaction between polarons, and larger multinucleon clusters must be considered. In particular, while we have addressed bound dineutrons only via the increased effective mass and the residual 1S_0 neutron-neutron interaction, the alpha-mediated interaction would further induce a larger dineutron binding energy as in the case of bipolarons [71,80–84].

The extension to the medium system with quartet condensation or quartet BCS models [85–90] would also be a fascinating direction. Moreover, the enhanced effective mass may lead to multinucleon clusters [14–16].

ACKNOWLEDGMENTS

H.T. is grateful to S. Furusawa for a useful discussion on supernova matter. This work is supported by Grants-in-Aid for Scientific Research provided by JSPS through Grants No. JP18H05406, No. JP22H01158, No. JP22H01214, No. JP22K13981, No. JP22K20372, No. JP23H01845, No. JP23H04526, No. JP23K03426, No. JP23K22485, No. JP23K25864, No. JP23K26538, No. JP24K17057, and No. JP24K06925. T.N. acknowledges the RIKEN Special Postdoctoral Researcher Program.

- [1] J. Blaizot, Nuclear compressibilities, *Phys. Rep.* **64**, 171 (1980).
- [2] H. Heiselberg, C. J. Pethick, and D. G. Ravenhall, Instabilities in hot nuclear matter: A mechanism for nuclear fragmentation, *Phys. Rev. Lett.* **61**, 818 (1988).
- [3] M. Pfützner, M. Karny, L. V. Grigorenko, and K. Riisager, Radioactive decays at limits of nuclear stability, *Rev. Mod. Phys.* **84**, 567 (2012).
- [4] M. Oertel, M. Hempel, T. Klähn, and S. Typel, Equations of state for supernovae and compact stars, *Rev. Mod. Phys.* **89**, 015007 (2017).
- [5] L. M. Satarov, I. N. Mishustin, A. Motornenko, V. Vovchenko, M. I. Gorenstein, and H. Stoecker, Phase transitions and Bose-Einstein condensation in α -nucleon matter, *Phys. Rev. C* **99**, 024909 (2019).
- [6] L. M. Satarov, M. I. Gorenstein, I. N. Mishustin, and H. Stoecker, Possible Bose-Einstein condensation of α particles in the ground state of nuclear matter, *Phys. Rev. C* **101**, 024913 (2020).
- [7] S. Furusawa and I. Mishustin, Degeneracy effects and Bose condensation in warm nuclear matter with light and heavy clusters, *Nucl. Phys. A* **1002**, 121991 (2020).
- [8] L. M. Satarov, R. V. Poberezhnyuk, I. N. Mishustin, and H. Stoecker, Phase diagram of α matter with a Skyrme-like scalar interaction, *Phys. Rev. C* **103**, 024301 (2021).
- [9] F. Hoyle, Resonances and nuclear molecular configurations in heavy-ion reactions, *Astrophys. J. Suppl.* **1**, 12 (1954).
- [10] A. Tohsaki, H. Horiuchi, P. Schuck, and G. Röpke, Alpha cluster condensation in ^{12}C and ^{16}O , *Phys. Rev. Lett.* **87**, 192501 (2001).
- [11] Y. Funaki, T. Yamada, H. Horiuchi, G. Röpke, P. Schuck, and A. Tohsaki, α -particle condensation in ^{16}O studied with a full four-body orthogonality condition model calculation, *Phys. Rev. Lett.* **101**, 082502 (2008).
- [12] T. Wakasa, E. Ihara, K. Fujita, Y. Funaki, K. Hatanaka, H. Horiuchi, M. Itoh, J. Kamiya, G. Röpke, H. Sakaguchi, N. Sakamoto, Y. Sakemi, P. Schuck, Y. Shimizu, M. Takashina, S. Terashima, A. Tohsaki, M. Uchida, H. Yoshida, and M. Yosoi, New candidate for an alpha cluster condensed state in $^{16}\text{O}(\alpha, \alpha')$ at 400 MeV, *Phys. Lett. B* **653**, 173 (2007).
- [13] S. Adachi, Y. Fujikawa, T. Kawabata, H. Akimune, T. Doi, T. Furuno, T. Harada, K. Inaba, S. Ishida, M. Itoh, C. Iwamoto, N. Kobayashi, Y. Maeda, Y. Matsuda, M. Murata, S. Okamoto, A. Sakaue, R. Sekiya, A. Tamii, and M. Tsumura, Candidates for the 5α condensed state in ^{20}Ne , *Phys. Lett. B* **819**, 136411 (2021).
- [14] K. Kisamori, S. Shimoura, H. Miya, S. Michimasa, S. Ota, M. Assie, H. Baba, T. Baba, D. Beaumel, M. Dozono, T. Fujii, N. Fukuda, S. Go, F. Hammache, E. Ideguchi, N. Inabe, M. Itoh, D. Kameda, S. Kawase, T. Kawabata *et al.*, Candidate resonant tetraneutron state populated by the $^4\text{He}(^8\text{He}, ^8\text{Be})$ reaction, *Phys. Rev. Lett.* **116**, 052501 (2016).

- [15] T. Faestermann, A. Bergmaier, R. Gernhäuser, D. Koll, and M. Mahgoub, Indications for a bound tetraneutron, *Phys. Lett. B* **824**, 136799 (2022).
- [16] M. Duer, T. Aumann, R. Gernhäuser, V. Panin, S. Paschalis, D. Rossi, N. Achouri, D. Ahn, H. Baba, C. Bertulani *et al.*, Observation of a correlated free four-neutron system, *Nature (London)* **606**, 678 (2022).
- [17] K. Miki *et al.* (RIBF-SHARAQ11 Collaboration and RCNP-E502 Collaboration), Precise spectroscopy of the $3n$ and $3p$ systems via the ${}^3\text{H}(t, {}^3\text{He})3n$ and ${}^3\text{He}({}^3\text{He}, t)3p$ reactions at intermediate energies, *Phys. Rev. Lett.* **133**, 012501 (2024).
- [18] A. M. Shirokov, G. Papadimitriou, A. I. Mazur, I. A. Mazur, R. Roth, and J. P. Vary, Prediction for a four-neutron resonance, *Phys. Rev. Lett.* **117**, 182502 (2016).
- [19] S. Gandolfi, H.-W. Hammer, P. Klos, J. E. Lynn, and A. Schwenk, Is a trineutron resonance lower in energy than a tetraneutron resonance? *Phys. Rev. Lett.* **118**, 232501 (2017).
- [20] R. Lazauskas, E. Hiyama, and J. Carbonell, Low energy structures in nuclear reactions with $4n$ in the final state, *Phys. Rev. Lett.* **130**, 102501 (2023).
- [21] F. M. Marqués and J. Carbonell, The quest for light multineutron systems, *Eur. Phys. J. A* **57**, 105 (2021).
- [22] H.-W. Hammer, C. Ji, and D. R. Phillips, Effective field theory description of halo nuclei, *J. Phys. G: Nucl. Part. Phys.* **44**, 103002 (2017).
- [23] I. Tanihata, H. Hamagaki, O. Hashimoto, Y. Shida, N. Yoshikawa, K. Sugimoto, O. Yamakawa, T. Kobayashi, and N. Takahashi, Measurements of interaction cross sections and nuclear radii in the light p -shell region, *Phys. Rev. Lett.* **55**, 2676 (1985).
- [24] I. Tanihata, M. Alcorta, D. Bandyopadhyay, R. Bieri, L. Buchmann, B. Davids, N. Galinski, D. Howell, W. Mills, S. Mythili, R. Openshaw, E. Padilla-Rodal, G. Ruprecht, G. Sheffer, A. C. Shotter, M. Trinczek, P. Walden, H. Savajols, T. Roger, M. Caamano *et al.*, Measurement of the two-halo neutron transfer reaction ${}^1\text{H}({}^{11}\text{Li}, {}^9\text{Li}){}^3\text{H}$ at 3A MeV, *Phys. Rev. Lett.* **100**, 192502 (2008).
- [25] M. Labiche, N. A. Orr, F. M. Marqués, J. C. Angélique, L. Axelsson, B. Benoit, U. C. Bergmann, M. J. G. Borge, W. N. Catford, S. P. G. Chappell, N. M. Clarke, G. Costa, N. Curtis, A. D'Arrigo, E. de Góes Brennand, O. Dorvaux, G. Fazio, M. Freer, B. R. Fulton, G. Giardina *et al.*, Halo structure of ${}^{14}\text{Be}$, *Phys. Rev. Lett.* **86**, 600 (2001).
- [26] K. J. Cook, T. Nakamura, Y. Kondo, K. Hagino, K. Ogata, A. T. Saito, N. L. Achouri, T. Aumann, H. Baba, F. Delaunay, Q. Deshayes, P. Doornenbal, N. Fukuda, J. Gibelin, J. W. Hwang, N. Inabe, T. Isobe, D. Kameda, D. Kanno, S. Kim *et al.*, Halo structure of the neutron-dripline nucleus ${}^{19}\text{B}$, *Phys. Rev. Lett.* **124**, 212503 (2020).
- [27] W. Horiuchi and Y. Suzuki, ${}^{22}\text{C}$: An s -wave two-neutron halo nucleus, *Phys. Rev. C* **74**, 034311 (2006).
- [28] K. Tanaka, T. Yamaguchi, T. Suzuki, T. Ohtsubo, M. Fukuda, D. Nishimura, M. Takechi, K. Ogata, A. Ozawa, T. Izumikawa, T. Aiba, N. Aoi, H. Baba, Y. Hashizume, K. Inafuku, N. Iwasa, K. Kobayashi, M. Komuro, Y. Kondo, T. Kubo *et al.*, Observation of a large reaction cross section in the drip-line nucleus ${}^{22}\text{C}$, *Phys. Rev. Lett.* **104**, 062701 (2010).
- [29] Y. Togano, T. Nakamura, Y. Kondo, J. Tostevin, A. Saito, J. Gibelin, N. Orr, N. Achouri, T. Aumann, H. Baba, F. Delaunay, P. Doornenbal, N. Fukuda, J. Hwang, N. Inabe, T. Isobe, D. Kameda, D. Kanno, S. Kim, N. Kobayashi *et al.*, Interaction cross section study of the two-neutron halo nucleus ${}^{22}\text{C}$, *Phys. Lett. B* **761**, 412 (2016).
- [30] T. Nagahisa and W. Horiuchi, Examination of the ${}^{22}\text{C}$ radius determination with interaction cross sections, *Phys. Rev. C* **97**, 054614 (2018).
- [31] J. Singh, J. Casal, W. Horiuchi, L. Fortunato, and A. Vitturi, Exploring two-neutron halo formation in the ground state of ${}^{29}\text{F}$ within a three-body model, *Phys. Rev. C* **101**, 024310 (2020).
- [32] S. Bagchi, R. Kanungo, Y. K. Tanaka, H. Geissel, P. Doornenbal, W. Horiuchi, G. Hagen, T. Suzuki, N. Tsunoda, D. S. Ahn, H. Baba, K. Behr, F. Browne, S. Chen, M. L. Cortés, A. Estradé, N. Fukuda, M. Holl, K. Itahashi, N. Iwasa *et al.*, Two-neutron halo is unveiled in ${}^{29}\text{F}$, *Phys. Rev. Lett.* **124**, 222504 (2020).
- [33] Z. H. Yang, Y. L. Ye, B. Zhou, H. Baba, R. J. Chen, Y. C. Ge, B. S. Hu, H. Hua, D. X. Jiang, M. Kimura, C. Li, K. A. Li, J. G. Li, Q. T. Li, X. Q. Li, Z. H. Li, J. L. Lou, M. Nishimura, H. Otsu, D. Y. Pang *et al.*, Observation of the exotic 0_2^+ cluster state in ${}^8\text{He}$, *Phys. Rev. Lett.* **131**, 242501 (2023).
- [34] Y. Yamaguchi, W. Horiuchi, T. Ichikawa, and N. Itagaki, Dineutron-dineutron correlation in ${}^8\text{He}$, *Phys. Rev. C* **108**, L011304 (2023).
- [35] J. Tanaka, Z. Yang, S. Typel, S. Adachi, S. Bai, P. van Beek, D. Beaumel, Y. Fujikawa, J. Han, S. Heil *et al.*, Formation of α clusters in dilute neutron-rich matter, *Science* **371**, 260 (2021).
- [36] L. D. Landau, Electron motion in crystal lattices, *Phys. Z. Sowjetunion* **3**, 664 (1933).
- [37] L. D. Landau and S. I. Pekar, Effective mass of a polaron, *Zh. Eksp. Teor. Fiz.* **18**, 419 (1948).
- [38] C. Baroni, G. Lamporesi, and M. Zaccanti, Quantum mixtures of ultracold gases of neutral atoms, *Nat. Rev. Phys.* **6**, 736 (2024).
- [39] E. Nakano, K. Iida, and W. Horiuchi, Quasiparticle properties of a single α particle in cold neutron matter, *Phys. Rev. C* **102**, 055802 (2020).
- [40] H. Moriya, H. Tajima, W. Horiuchi, K. Iida, and E. Nakano, Binding two and three α particles in cold neutron matter, *Phys. Rev. C* **104**, 065801 (2021).
- [41] H. Tajima, H. Moriya, W. Horiuchi, E. Nakano, and K. Iida, Intersections of ultracold atomic polarons and nuclear clusters: How is a chart of nuclides modified in dilute neutron matter? *AAPPS Bulletin* **34**, 9 (2024).
- [42] H. Tajima, H. Moriya, W. Horiuchi, E. Nakano, and K. Iida, Polaronic proton and diproton clustering in neutron-rich matter, *Phys. Lett. B* **851**, 138567 (2024).
- [43] M.-G. Hu, M. J. Van de Graaff, D. Kedar, J. P. Corson, E. A. Cornell, and D. S. Jin, Bose polarons in the strongly interacting regime, *Phys. Rev. Lett.* **117**, 055301 (2016).
- [44] N. B. Jorgensen, L. Wacker, K. T. Skalmstang, M. M. Parish, J. Levinsen, R. S. Christensen, G. M. Bruun, and J. J. Arlt, Observation of attractive and repulsive polarons in a Bose-Einstein condensate, *Phys. Rev. Lett.* **117**, 055302 (2016).
- [45] Z. Z. Yan, Y. Ni, C. Robens, and M. W. Zwierlein, Bose polarons near quantum criticality, *Science* **368**, 190 (2020).
- [46] M. Duda, X.-Y. Chen, A. Schindewolf, R. Bause, J. von Milczewski, R. Schmidt, I. Bloch, and X.-Y. Luo, Transition from a polaronic condensate to a degenerate Fermi gas of heteronuclear molecules, *Nat. Phys.* **19**, 720 (2023).
- [47] S. P. Rath and R. Schmidt, Field-theoretical study of the Bose polaron, *Phys. Rev. A* **88**, 053632 (2013).

- [48] J. Levinsen, M. M. Parish, and G. M. Bruun, Impurity in a Bose-Einstein condensate and the Efimov effect, *Phys. Rev. Lett.* **115**, 125302 (2015).
- [49] F. Grusdt, R. Schmidt, Y. E. Shchadilova, and E. Demler, Strong-coupling Bose polarons in a Bose-Einstein condensate, *Phys. Rev. A* **96**, 013607 (2017).
- [50] L. A. Peña Ardila, N. B. Jørgensen, T. Pohl, S. Giorgini, G. M. Bruun, and J. J. Arlt, Analyzing a Bose polaron across resonant interactions, *Phys. Rev. A* **99**, 063607 (2019).
- [51] J. Takahashi, R. Imai, E. Nakano, and K. Iida, Bose polaron in spherical trap potentials: Spatial structure and quantum depletion, *Phys. Rev. A* **100**, 023624 (2019).
- [52] S. I. Mistakidis, G. C. Katsimiga, G. M. Koutentakis, T. Busch, and P. Schmelcher, Quench dynamics and orthogonality catastrophe of Bose polarons, *Phys. Rev. Lett.* **122**, 183001 (2019).
- [53] N.-E. Guenther, P. Massignan, M. Lewenstein, and G. M. Bruun, Bose polarons at finite temperature and strong coupling, *Phys. Rev. Lett.* **120**, 050405 (2018).
- [54] F. Isaule, I. Morera, P. Massignan, and B. Juliá-Díaz, Renormalization-group study of Bose polarons, *Phys. Rev. A* **104**, 023317 (2021).
- [55] H. Tajima, J. Takahashi, S. I. Mistakidis, E. Nakano, and K. Iida, Polaron problems in ultracold atoms: Role of a Fermi sea across different spatial dimensions and quantum fluctuations of a Bose medium, *Atoms* **9**, 18 (2021).
- [56] F. Scazza, M. Zaccanti, P. Massignan, M. M. Parish, and J. Levinsen, Repulsive Fermi and Bose polarons in quantum gases, *Atoms* **10**, 55 (2022).
- [57] Z. Li, S. Singh, T. V. Tscherbul, and K. W. Madison, Feshbach resonances in ultracold ^{85}Rb - ^{87}Rb and ^6Li - ^{87}Rb mixtures, *Phys. Rev. A* **78**, 022710 (2008).
- [58] C.-H. Wu, I. Santiago, J. W. Park, P. Ahmadi, and M. W. Zwierlein, Strongly interacting isotopic Bose-Fermi mixture immersed in a Fermi sea, *Phys. Rev. A* **84**, 011601(R) (2011).
- [59] J. W. Park, C.-H. Wu, I. Santiago, T. G. Tiecke, S. Will, P. Ahmadi, and M. W. Zwierlein, Quantum degenerate Bose-Fermi mixture of chemically different atomic species with widely tunable interactions, *Phys. Rev. A* **85**, 051602(R) (2012).
- [60] M. Repp, R. Pires, J. Ulmanis, R. Heck, E. D. Kuhnle, M. Weidemüller, and E. Tiemann, Observation of interspecies ^6Li - ^{133}Cs Feshbach resonances, *Phys. Rev. A* **87**, 010701 (2013).
- [61] M. M. Forbes, A. Gezerlis, K. Hebeler, T. Lesinski, and A. Schwenk, Neutron polaron as a constraint on nuclear density functionals, *Phys. Rev. C* **89**, 041301(R) (2014).
- [62] I. Vidaña, Fermi polaron in low-density spin-polarized neutron matter, *Phys. Rev. C* **103**, L052801 (2021).
- [63] H. Tajima, H. Funaki, Y. Sekino, N. Yasutake, and M. Matsuo, Exploring 3P_0 superfluid in dilute spin-polarized neutron matter, *Phys. Rev. C* **108**, L052802 (2023).
- [64] J. Levinsen, P. Massignan, F. Chevy, and C. Lobo, p -wave polaron, *Phys. Rev. Lett.* **109**, 075302 (2012).
- [65] Y. Ma and X. Cui, Highly polarized one-dimensional Fermi gases near a narrow p -wave resonance, *Phys. Rev. A* **100**, 062712 (2019).
- [66] O. I. Utesov and S. V. Andreev, Magnetoroton in a two-dimensional Bose-Bose mixture, *Phys. Rev. B* **109**, 235135 (2024).
- [67] M. Matsuo, Spatial structure of neutron Cooper pair in low density uniform matter, *Phys. Rev. C* **73**, 044309 (2006).
- [68] H. Tajima, H. Moriya, W. Horiuchi, K. Iida, and E. Nakano, Resonance-to-bound transition of ^5He in neutron matter and its analogy with heteronuclear Feshbach molecules, *Phys. Rev. C* **106**, 045807 (2022).
- [69] In Ref. [68], the neutron and alpha-particle momenta in the center-of-mass frame were wrongly taken as $\mathbf{k} + \mathbf{P}/2$ and $-\mathbf{k} + \mathbf{P}/2$, respectively. Since only the case with $\mathbf{P} = \mathbf{0}$ was considered in Ref. [68], however, the results were not affected by this choice at all.
- [70] K. Nishimura, E. Nakano, K. Iida, H. Tajima, T. Miyakawa, and H. Yabu, Ground state of the polaron in an ultracold dipolar Fermi gas, *Phys. Rev. A* **103**, 033324 (2021).
- [71] A. Camacho-Guardian, L. A. Peña Ardila, T. Pohl, and G. M. Bruun, Bipolarons in a Bose-Einstein condensate, *Phys. Rev. Lett.* **121**, 013401 (2018).
- [72] L. A. P. Ardila and S. Giorgini, Impurity in a Bose-Einstein condensate: Study of the attractive and repulsive branch using quantum Monte Carlo methods, *Phys. Rev. A* **92**, 033612 (2015).
- [73] O. I. Utesov, M. I. Baglay, and S. V. Andreev, Effective interactions in a quantum Bose-Bose mixture, *Phys. Rev. A* **97**, 053617 (2018).
- [74] W. Li and X. Cui, Repulsive Fermi polarons with negative effective mass, *Phys. Rev. A* **96**, 053609 (2017).
- [75] J. W. Clark and E. Krotscheck, Alpha matter revisited, [arXiv:2304.08543](https://arxiv.org/abs/2304.08543).
- [76] Y. Funaki, H. Horiuchi, W. von Oertzen, G. Röpke, P. Schuck, A. Tohsaki, and T. Yamada, Concepts of nuclear α -particle condensation, *Phys. Rev. C* **80**, 064326 (2009).
- [77] P. van Wyk, H. Tajima, D. Inotani, A. Ohnishi, and Y. Ohashi, Superfluid Fermi atomic gas as a quantum simulator for the study of the neutron-star equation of state in the low-density region, *Phys. Rev. A* **97**, 013601 (2018).
- [78] N. Itagaki and S. Okabe, Molecular orbital structures in ^{10}Be , *Phys. Rev. C* **61**, 044306 (2000).
- [79] M. Dan, R. Chatterjee, and M. Kimura, A description of the structure and electromagnetic breakup of ^{11}Be with microscopic inputs, *Eur. Phys. J. A* **57**, 203 (2021).
- [80] P. Naidon, Two impurities in a Bose-Einstein condensate: From Yukawa to Efimov attracted polarons, *J. Phys. Soc. Jpn.* **87**, 043002 (2018).
- [81] G. Panochko and V. Pastukhov, Two- and three-body effective potentials between impurities in ideal BEC, *J. Phys. A: Math. Theor.* **54**, 085001 (2021).
- [82] K. Fujii, M. Hongo, and T. Enss, Universal van der Waals force between heavy polarons in superfluids, *Phys. Rev. Lett.* **129**, 233401 (2022).
- [83] R. Paredes, G. Bruun, and A. Camacho-Guardian, Perspective: Interactions mediated by atoms, photons, electrons, and excitons, *Phys. Rev. A* **110**, 030101 (2024).
- [84] E. Nakano, T. Miyakawa, and H. Yabu, Two-body problem of impurity atoms in dipolar Fermi gas, [arXiv:2404.14866](https://arxiv.org/abs/2404.14866).
- [85] G. Röpke, A. Schnell, P. Schuck, and P. Nozières, Four-particle condensate in strongly coupled fermion systems, *Phys. Rev. Lett.* **80**, 3177 (1998).
- [86] N. Sandulescu, D. Negrea, J. Dukelsky, and C. W. Johnson, Quartet condensation and isovector pairing correlations in $N=Z$ nuclei, *Phys. Rev. C* **85**, 061303(R) (2012).

- [87] R. Sen'kov and V. Zelevinsky, Unified BCS-like model of pairing and alpha-correlations, *Phys. At. Nucl.* **74**, 1267 (2011).
- [88] N. Sandulescu, D. Negrea, and D. Gambacurta, Proton-neutron pairing in $N = Z$ nuclei: Quartetting versus pair condensation, *Phys. Lett. B* **751**, 348 (2015).
- [89] V. Baran and D. Delion, A quartet BCS-like theory, *Phys. Lett. B* **805**, 135462 (2020).
- [90] Y. Guo, H. Tajima, and H. Liang, Cooper quartet correlations in infinite symmetric nuclear matter, *Phys. Rev. C* **105**, 024317 (2022).